
Feedback Descent: Open-Ended Text Optimization via Pairwise Comparison

Yoonho Lee¹, Joseph Boen¹, Chelsea Finn¹

¹Stanford University

Abstract. We introduce *Feedback Descent*, a framework that optimizes text artifacts—prompts, code, and molecules—through structured textual feedback rather than relying solely on scalar rewards. By preserving detailed critiques instead of compressing them to binary preferences, *Feedback Descent* widens the information bottleneck in preference learning, enabling directed optimization in text space rather than weight space. We show that in-context learning can transform structured feedback into gradient-like directional information, enabling targeted edits. Unlike prior approaches that collapse judgments into single bits, our evaluators pair each comparison with textual feedback, which functions as high-bandwidth supervision. The iteration loop is done purely at inference time, without modifying any model weights, and is task-agnostic. We evaluate *Feedback Descent* on three diverse domains and find that it outperforms state-of-the-art prompt optimization (GEPA), reinforcement learning methods (GRPO, REINVENT), and even specialized graph-based molecular optimizers. In the DOCKSTRING molecule discovery benchmark, *Feedback Descent* identifies novel drug-like molecules surpassing the 99.9th percentile of a database with more than 260,000 compounds across six protein targets.

1. Introduction

A central goal of machine learning is building systems that can perform tasks beyond human capabilities. Reinforcement learning is a powerful framework that accomplishes this goal, since it can optimize with respect to feedback on its own outputs, rather than relying on supervised examples of desired outputs. Indeed, recent language models have demonstrated impressive feats in domains like math and programming [12, 17, 52, 93] through a combination of reinforcement learning and text-based reasoning. Unfortunately, existing reinforcement learning frameworks are designed to learn from impoverished supervision signals, typically either scalar rewards or pairwise preference data, where each annotation conveys at most a single bit per pair. These bottlenecks discard information about *why* one behavior is better and *how* to improve—information available in environment feedback or easily elicited from humans during annotation [32, 80].

Our goal is to widen this information bottleneck, i.e., significantly increase the information the system can extract per unit of experience [66]. Collecting more detailed feedback is straightforward, e.g., with brief rationales explaining preferences; the challenge is turning such feedback into measurable improvement. Because free-form feedback does not define a differentiable objective, it cannot directly drive weight updates via backpropagation. Our approach iterates at inference time, using language models to translate accumulated feedback into targeted edits of text artifacts (prompts, code, molecules, JSON configs) that improve a final performance objective, without any weight updates.

To that end, we introduce *Feedback Descent*, a framework for continual optimization in text space. At each iteration, we prompt a language model to propose an improved version of the current best artifact, conditioned on all previous feedback. We compare this candidate against the current best, and the evaluator returns a preference along with textual feedback explaining the choice. If the candidate is preferred, it becomes the new best. Repeating this loop yields semantically local, feedback-aligned improvements that implement gradient-like steps in text space. See Figure 1 for a conceptual illustration. We provide theoretical intuition for why *Feedback Descent* can be effective. Under appropriate assumptions about feedback quality and problem structure, we demonstrate that textual feedback can provide directional information, enabling efficient optimization.

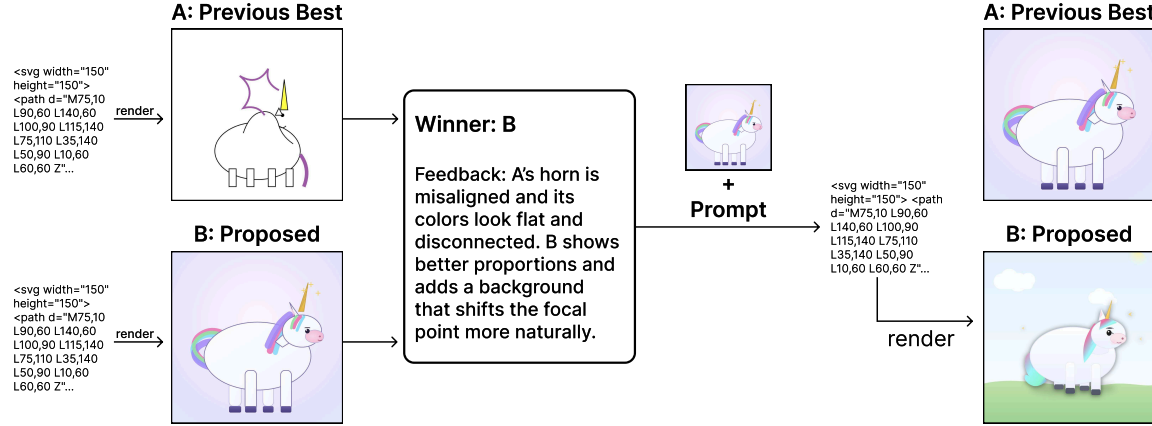


Figure 1: A conceptual illustration of feedback descent. At each iteration, we compare the previous best artifact with a new candidate. The evaluator provides both a pairwise preference and textual feedback. Preferences ensure the selection of better candidates, while feedback accumulates directional information that guides semantically meaningful edits.

Our contributions are threefold. **First**, we formalize why textual feedback enables dimension-free convergence while zeroth-order methods suffer exponential slowdown with effective dimensionality, identifying when and why structured feedback outperforms scalar rewards. **Second**, we demonstrate cross-domain generality: Feedback Descent works across three qualitatively distinct domains (visual design, prompt optimization, molecule design) with the same iterative loop. **Third**, we validate competitive or superior performance versus specialized methods, achieving competitive results with the state-of-the-art in prompt optimization (GEPA) while outperforming a reinforcement learning baseline (GRPO). In the molecule design experiment, Feedback Descent outperforms specialized molecular optimizers (Graph MCTS/GA, REINVENT) despite operating purely on text representations, discovering molecules that surpass the 99.9th percentile of a 260,000-compound database of molecules.

2. Feedback Descent: Open-Ended Text Optimization

We propose Feedback Descent, a framework for open-ended optimization of text-representable artifacts whose quality is easier to *judge* than to *construct*. Feedback Descent converts comparative textual feedback into directed semantic edits and iterates in a self-improvement loop. As a running example, consider optimizing SVG code to render better images of a unicorn. Current vision-language models can reliably compare two renderings and explain the choice, even if writing high-quality SVG from scratch is difficult. Through Feedback Descent, we can convert these explanations into directed edits that aim to produce an artifact that surpasses all previous ones.

2.1. Problem Setup

Let \mathcal{S} be the space of token sequences, and let $x \in \mathcal{S}$ denote an artifact (e.g., SVG code). Given the current best $x_t^* \in \mathcal{S}$ and a candidate $x \in \mathcal{S}$, the evaluator returns

$$E(x, x_t^*) \rightarrow (p \in \{0, 1\}, r \in \mathcal{S}), \quad (1)$$

where $p = 1$ indicates $x \succ x_t^*$ and r is a textual feedback explaining *why* the winner is better and *how* to improve. We append r_t to a history $\mathcal{R}_t = \{(x_1, r_1), \dots, (x_t, r_t)\}$ and iterate, keeping track of the current best artifact x_t^* .

2.2. Feedback Descent

Feedback Descent operates as an iterative optimization loop that maintains a single best artifact x_t^* and progressively improves it through feedback-guided mutations and comparative evaluation. Throughout, we use \mathcal{M} to denote the language model used for generating improved candidates.

Initialization and termination. We initialize x_0^* by prompting a language model with the task description alone (e.g., "Generate SVG code for a unicorn"). The algorithm runs for a fixed budget of T iterations or until convergence (defined as no improvement for k consecutive iterations).

Proposing semantic mutations via prompting. The mutation step leverages a language model's in-context learning capabilities. At iteration t , we prompt the model with the current best artifact x_t^* and accumulated feedback \mathcal{R}_{t-1} to generate an improved candidate:

$$x_t = \mathcal{M}(x_t^*, \mathcal{R}_{t-1}) \quad (2)$$

The prompt instructs the model to address previous critiques while preserving successful elements. These prompts are intentionally minimal: the optimization signal comes from the accumulated feedback rather than heavy prompt engineering.

They include basic task context, the current best artifact, and feedback from previous comparisons. Complete prompt templates for each domain are provided in Section C.3.

Selection and update. We compare the new candidate x_t against the current best x_t^* using the evaluator $E(x_t, x_t^*)$, which returns both a binary preference p_t and a textual feedback r_t . In our running SVG example, examples of feedback include "adjust the stroke width", "make sure the legs are connected to the body", and "add a shadow to the unicorn's mane". Regardless of the preference outcome, we always add the feedback to our history: $\mathcal{R}_{t+1} = \mathcal{R}_t \cup \{(x_t, r_t)\}$. If $p_t = 1$ (candidate is preferred), we update $x_{t+1}^* = x_t$; otherwise we keep $x_{t+1}^* = x_t^*$. We summarize the overall process in Algorithm 1.

2.3. Analogy to Gradient Descent

The key algorithmic insight is best understood by analogy to the gradient descent algorithm. Just as gradients provide the direction of steepest ascent under local linearity, textual feedback can suggest plausible directions of improvement in semantic space. For our SVG example, if the feedback indicates "needs more defined horn shape," we expect that a small edit to the horn shape that preserves overall structure will likely be an improvement.

Of course, textual feedback is not a literal gradient. It is approximate and occasionally contradictory—optimization with such feedback does not have convergence guarantees in the same way that gradient descent does. Instead, feedback acts as a heuristic directional cue, offering higher-bandwidth supervision than a binary preference signal or a scalar reward, just as first-order optimization is fundamentally faster than zeroth-order optimization [1, 47, 48]. We hypothesize that an open-ended optimization loop based on such cues can succeed, supported by prior evidence that language models reliably translate textual instructions into concrete modifications. Examples include generating code changes [4, 9, 16, 27, 41, 50, 60, 74], following complex multi-step instructions [14, 40, 54, 75, 91], targeted text modifications [18, 42, 44, 63, 78], and decomposing high-level goals into executable action sequences [2, 55, 58, 64, 73, 87].

Why directional information helps. Zeroth-order methods that rely only on function evaluations or binary preferences suffer severe dimension-dependent slowdowns: convergence rates degrade exponentially as the search space grows [47, 48]. In contrast, first-order methods exploit gradient information to achieve dimension-free convergence under standard assumptions. Textual feedback provides an approximation to such directional in-

Algorithm 1 Feedback Descent

Require: Initial text x_0 , Language model \mathcal{M} , T

- 1: Current best: $x^* \leftarrow x_0$, Rationale history: $\mathcal{R} \leftarrow \emptyset$
- 2: **for** $t = 1$ to T **do**
- 3: $x_t \leftarrow \mathcal{M}(x^*, \mathcal{R})$ ▷ Propose (2)
- 4: $p_t, r_t \leftarrow \text{COMPARE}(x_t, x^*)$ ▷ Compare (1)
- 5: $\mathcal{R} \leftarrow \mathcal{R} \cup \{(x_t, r_t)\}$
- 6: **if** $p_t = 1$ **then**
- 7: $x^* \leftarrow x_t, \mathcal{R} \leftarrow \emptyset$ ▷ Update + reset
- 8: **return** x^*

formation. Even when individual rationales are imperfect, their aggregate message across failures continually refines the direction of improvement. We formalize this intuition in Section A, showing that under idealized assumptions, rationale-guided updates can achieve linear convergence rates independent of effective dimensionality, while zeroth-order baselines scale exponentially worse. These results provide motivation rather than rigorous guarantees for the discrete text domains we study empirically. In Section 4, we show that Feedback Descent indeed produces consistent improvements across tasks, validating that such heuristic directional cues are sufficient to drive open-ended text optimization.

3. Related Work

Preference Learning. Preference learning methods learn from pairwise comparisons [5, 13, 19, 46, 54]; recent advances include bypassing the need for a reward model [59], iterative optimization under KL constraints [81], and adaptive scaling techniques [72]. However, these methods fundamentally compress complex human reasoning into binary or scalar preferences, thereby forgoing the rich explanatory content that humans can naturally provide alongside their judgments [79]. Recent work shows that fine-grained feedback significantly improves reward modeling [80, 88], and incorporating rationales alongside preferences provides richer training signals [32]. Unlike prior work that uses rationales to improve weight-based training, we leverage detailed textual feedback entirely at inference time, widening the information bottleneck without requiring retraining.

Evolutionary Algorithms and Gradient-Free Optimization. Feedback Descent can be viewed as an evolutionary algorithm [26, 29], in which candidates are iteratively mutated and accepted based on fitness. While the black-box nature of modern LLMs has spurred interest in applying gradient-free approaches [11, 28, 37, 68], these methods face fundamental challenges in high-dimensional spaces. More broadly, zeroth-order methods [10] face convergence rates that scale poorly with dimension, which is consistent with our experimental results comparing with reinforcement learning methods in Section 4. To our best knowledge, Wang et al. [71] was the first prior work to demonstrate that LLMs can be effective molecule optimizers inside evolutionary algorithm loops. Feedback Descent explores whether textual rationales can provide useful directional information for optimization, similar to how Nie et al. [49] shows that LLMs can be effective optimizers when provided with directional feedback from historical traces. Our contribution is in operationalizing an effective *directed mutation operator* via accumulated textual feedback.

Optimizing Compound AI Systems. Compound AI systems, i.e., modular architectures involving multiple LLM invocations and complex control flow, such as agents or scaffolding techniques [87], present unique optimization challenges due to their modularity. Several approaches have emerged to tackle this complexity, including optimization for searching and bootstrapping few-shot in-context examples [33, 34, 53] and reflective prompt evolution [3]. The closest prior work to Feedback Descent is TextGrad [89], which proposes PyTorch-like framework for automatic differentiation via text, backpropagating textual gradients through computation graphs. A core difference is that TextGrad optimizes “pointwise”, i.e., it proposes a new instance of the artifact based only on the latest one. In contrast, Feedback Descent keeps an explicit trajectory-level buffer of comparative feedback. As we will see in Section 4, Feedback Descent is much more scalable at long-horizon optimization compared to TextGrad.

Inference-Time Optimization for LLMs. Inference-time optimization improves performance without weight updates by performing additional computation at generation. This paradigm includes self-critique and refinement cycles (constitution-guided critique [6]; Self-Refine [42]) test-time scaling via best-of- N , multi-step reasoning, and tree search [15, 86, 90], and iterative prompt optimization [56, 83, 92]. Several works report that strategically allocating inference-time compute yields large gains [24, 45, 67, 84].

We build on the growing consensus that natural language is a particularly powerful medium for inference-time improvement. Natural language traces enable models to reason effectively in complex environments [35, 76], and language models can reliably map textual instructions to concrete modifications [4, 9, 20, 61, 62]. However, existing methods often rely on random sampling of self-generated critiques, which may be noisy or fail to capture external preferences. In contrast, we leverage external rationales as directional information, enabling guided

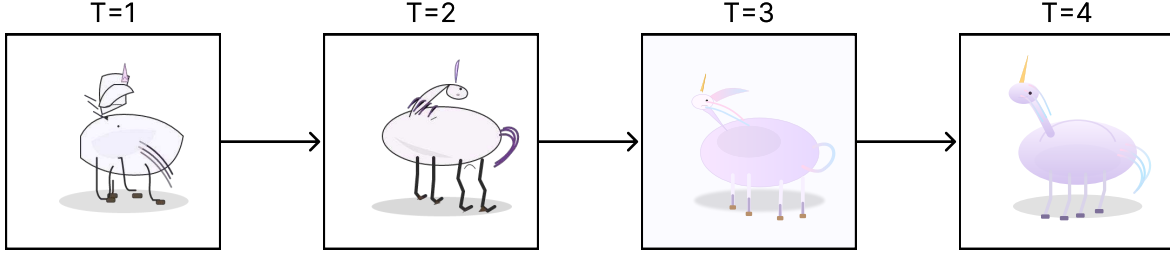


Figure 2: Iterative progression of SVG unicorn optimization under the realism judge. **Feedback Descent produces gradual, semantically meaningful improvements through accumulating directional cues.**

Setup	Subject	Ink Wash	Minimalist	Realistic	Arcade	Stain Glass
From Scratch	City Skyline	100.0%	100.0%	100.0%	100.0%	100.0%
	Mushroom	100.0%	100.0%	83.3%	100.0%	100.0%
	Robot	100.0%	100.0%	100.0%	100.0%	100.0%
	Unicorn	100.0%	100.0%	100.0%	100.0%	100.0%
Judge-Aware	City Skyline	50.0%	100.0%	100.0%	100.0%	88.9%
	Mushroom	100.0%	100.0%	100.0%	100.0%	94.1%
	Robot	100.0%	100.0%	100.0%	93.8%	100.0%
	Unicorn	89.5%	100.0%	100.0%	93.8%	80.0%

Table 1: Win rates after five iterations comparing Feedback Descent against direct prompting under two conditions: *From Scratch* and *Aware* of the judge rubric. Feedback Descent matches or outperforms the baseline on all combinations tested (i.e. $\geq 50\%$). **Iterative feedback consistently improves SVG designs over direct prompting.**

search in the semantic space.

4. Experiments

We evaluate Feedback Descent across three diverse domains—visual design, prompt optimization, and molecule discovery—to demonstrate its generality and effectiveness. Our evaluation spans diverse representations and evaluation modalities: (1) **Representation diversity**: SVG (spatial/geometric), prompts (instructional text), molecules (chemical structures). (2) **Evaluation modality**: SVG uses vision-language model comparison, prompt optimization uses dataset-specific accuracy metrics, molecules use computational docking scores. Together, our experiments answer the question: *Can a single optimization framework, with no domain-specific engineering, match or exceed specialized methods purely through structured feedback?*

4.1. Experimental Domains

We describe each evaluation domain and how we obtain pairwise comparisons augmented with textual rationales.

SVG optimization. Taking inspiration from Bubeck et al. [8], we evaluate the ability of models to output SVG code for illustrations of unicorns. We use a set of five diverse judge prompts, each preferring a different aesthetic: *ink wash* painting style, *minimalist* design, *realism*, *retro arcade* pixel-art motifs, and *stained glass* artwork. We compare rendered SVGs using GPT-5-mini, which outputs both a binary preference and short textual feedback. To mitigate order bias, we perform two judgments with swapped image orders (A-B and B-A) and declare a winner only if both judgments are consistent. Otherwise, we try again, up to three times, and discard if no consistent winner emerges.

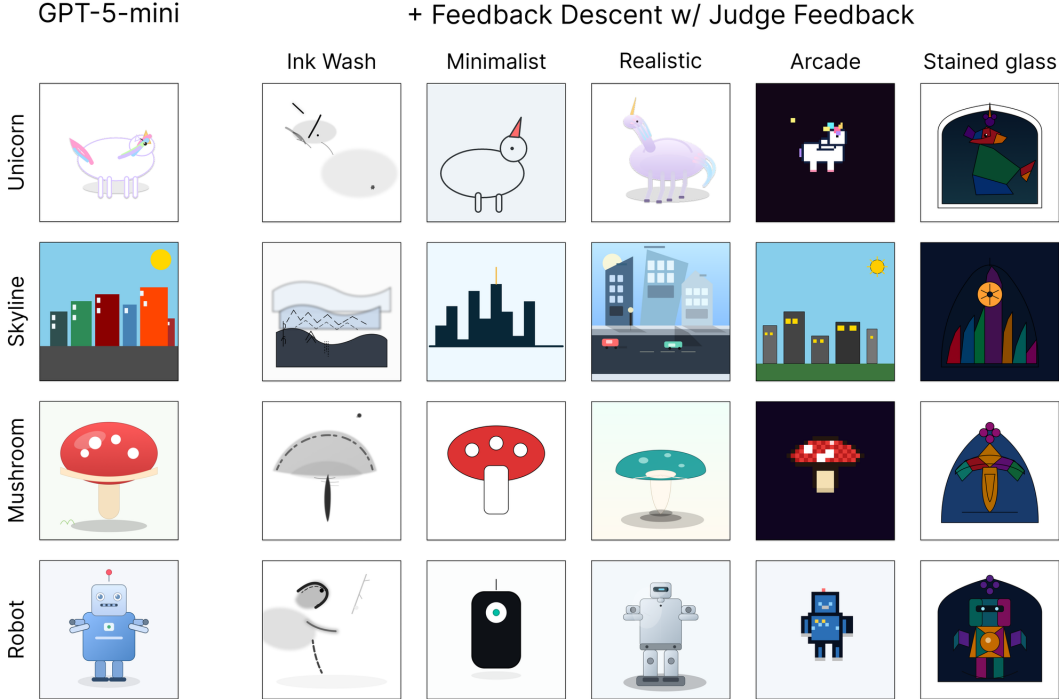


Figure 3: Example images generated by Feedback Descent under six different judge criteria. **Feedback Descent yields visually distinct objects aligned with the aesthetic criteria preferred by each judge.**

Prompt optimization. We follow the setup of GEPA [3] across four diverse tasks: multi-hop reasoning (HotpotQA; Yang et al. [85]), instruction following (IFBench; Pyatkin et al. [57]), privacy-aware delegation (PUPA; Li et al. [38]), and retrieval-augmented verification (HoVer; Jiang et al. [31]). We evaluate on both open-source (Qwen3-8B; Yang et al. [82]) and proprietary (GPT-4.1 mini) models. For each task, we use the same multi-stage programs from GEPA, where the number of stages differs across datasets, and we jointly optimize the prompts for all stages using Feedback Descent. Optimization is driven by training examples: candidate prompts are updated based on performance on the training set and textual feedback describing which constraints were satisfied or violated. All candidate prompts are scored on validation examples, and the prompt with the highest validation accuracy rate is selected. We report performance on held-out test examples.

Molecule discovery. We evaluate on molecular docking tasks using DOCKSTRING [22] docking scores and drug-likeness (QED). DOCKSTRING provides a realistic drug discovery setting where molecules are evaluated based on their predicted binding affinity to medically relevant targets, rather than relying solely on simple physicochemical properties. We focus on challenging optimization tasks across six protein targets: ADRB1, PGR, PPARA, PPARG, CDK2, and F2. Following DOCKSTRING, we compute the combined score $s = -\text{Vina} - 10 \times (1 - \text{QED})$. We represent molecules as SMILES strings [77] and evaluate using DOCKSTRING’s molecular docking pipeline to compute Vina scores (binding affinity). The feedback system provides rich structured information, including RDKit molecular descriptors [36], similarity searches against known compounds from molecular databases [23, 25, 39, 43], and detailed docking results. In the system prompt, we also provide the LLM information about the protein target obtained from the UniProt database [69]. Together, this provides the LLM with detailed feedback on molecular properties that affect binding affinity, drug-likeness violations, and comparisons to known active compounds.

4.2. SVG Optimization

We evaluate iterative feedback against direct prompting across two generators, GPT-4o-mini and GPT-5-mini. The direct prompting baseline receives the full evaluation rubric and is tasked with producing a single best design. Feedback Descent instead begins with an initial set of candidates, and through 5 rounds of structured feedback

Method	Qwen3-8B				GPT-4.1 Mini			
	HpQA	IFBench	Hover	PUPA	HpQA	IFBench	Hover	PUPA
DSPy Default [34]	42.33	36.90	35.33	80.82	38.00	47.79	46.33	78.57
MIPROv2 [53]	55.33	36.22	47.33	81.55	58.00	49.15	48.33	83.37
GRPO [65]	43.33	35.88	38.67	86.66	—	—	—	—
GEPA [3]	62.33	38.61	52.33	91.85	69.00	52.72	51.67	94.47
Feedback Descent (ours)	60.00	38.78	60.00	90.90	68.33	54.59	57.67	85.66

Table 2: Prompt optimization results across multiple benchmarks. Feedback Descent consistently outperforms or is competitive with state-of-the-art methods.

and improvement, refines designs using judge comparisons that reflect aesthetic criteria. We test two initialization regimes: **Scratch**, which starts from images simply instructed to generate images of unicorns, and **Informed**, which starts from the strongest direct generations conditioned on the rubric, determined by the LLM judge.

Results. Table 1 shows the win rates after 5 iterations. For both GPT-4o-mini and GPT-5-mini, Feedback Descent reliably improves outputs over the initial population. Furthermore, qualitative examples of an optimization trajectory in Figure 2 and each judge-object pair in Figure 3 demonstrate that the procedure consistently produces unicorns whose visual style diverges across judges, aligning with aesthetic criteria such as geometry, minimalism, or retro arcade motifs.

Iterative feedback can elicit better outputs from the same model

Because of a generator-verifier gap, even prompting with the exact judge rubric is suboptimal for SVG generation. Feedback Descent elicits better images from the same generator by iteratively proposing improvements guided by feedback.

4.3. Prompt Optimization

We compare Feedback Descent against five baselines: the default prompt implemented in the DSPy program [34, Default], a Bayesian optimization approach for selecting instructions and demonstrations [53, MIPROv2], online reinforcement learning [65, GRPO], and a reflective prompt evolution method [3, GEPA]. All baselines are run under matched rollout budgets for fair comparison, and the reported baseline results are from Agrawal et al. [3].

Each example produces pointwise feedback about which constraints were satisfied or violated. To construct the pairwise feedback for Feedback Descent, we stratify the examples into quadrants based on whether each prompt resulted in a correct response. We then ask the model to propose textual descriptions of inputs where these discrepancies arise. We then statistically validate each hypothesis, filtering for ones that correspond to consistent differences in performance between the prompts. This process distills the true global differences between the two prompts.

Table 2 shows that Feedback Descent is competitive with GEPA across both models, achieving the best performance on IFBench and Hover, while GEPA leads on HotpotQA and PUPA. Despite GEPA being specifically engineered for prompt optimization with coordinate descent and Pareto frontier maintenance, Feedback Descent achieves competitive performance with a simpler approach: jointly optimizing all prompts at once via automated textual summaries of pairwise performance differences. We do not claim to present a state-of-the-art prompt optimizer; rather, these results demonstrate that our general-purpose framework remains competitive with specialized methods while requiring minimal domain-specific engineering.

Method	ADRB1	PGR	PPARA	PPARG	CDK2	F2	Avg	
DOCKSTRING (N=260155)	Top 50%	5.305	3.478	4.549	4.210	4.385	4.168	4.349
	Top 90%	8.785	7.878	7.987	7.658	7.733	7.477	7.920
	Top 99%	9.620	8.703	8.718	8.449	8.453	8.139	8.680
	Top 99.9%	10.209	9.260	9.230	9.012	8.979	8.722	9.235
	Top 99.99%	<u>10.742</u>	<u>9.723</u>	9.821	9.518	9.509	9.252	9.761
	Best Molecule	<u>11.330</u>	<u>9.742</u>	9.907	9.529	9.534	<u>9.311</u>	9.892
Graph MCTS [†] [30]	8.883	7.819	7.363	7.134	7.777	6.310	7.548	
SMILES GA [7]	9.334	8.335	9.052	8.560	8.268	7.984	8.589	
REINVENT [51]	9.867	8.604	8.735	9.054	8.695	8.441	8.899	
Graph GA [†] [30]	10.249	8.793	9.211	8.769	8.652	8.900	9.096	
GP-BO [†] [70]	10.552	9.307	9.680	9.485	9.067	8.686	9.463	
TextGrad [89]	8.531	8.057	7.953	7.256	8.174	7.357	7.888	
Feedback Descent (ours)	10.623	9.615	9.919	10.187	9.803	9.300	9.908	
w/ No Feedback	6.190	8.619	8.230	8.633	8.300	8.793	8.127	
w/ Random Feedback	6.604	8.385	8.276	6.780	8.793	7.993	7.805	
w/ Binary Only	5.863	8.779	8.507	7.998	9.439	8.420	8.168	

Table 3: Results for molecule optimization on six protein targets. Full results with standard deviations are in Table 6. For each target, the top generative result is in **bold**, and any population in the DOCKSTRING database that exceeds the best generative result is underlined. **Feedback Descent** rivals or surpasses specialized molecular optimizers across all six targets.

Pairwise Comparisons Suffice for Competitive Prompt Optimization

Feedback Descent is competitive with GEPA, a state-of-the-art prompt optimization method, despite employing a simpler, domain-agnostic approach.

4.4. Molecule Optimization (DOCKSTRING)

We compare against baselines implemented in the `mol_opt` repository [21]. Our comparisons include a genetic algorithm [7, SMILES GA], reinforcement learning [51, REINVENT], fragment-based algorithms [30, Graph MCTS/GA], and Bayesian optimization on molecular graphs [70, GP-BO]. Because fragment-based methods exploit graph-level structural priors, the most direct comparison is to the text-only baselines: SMILES-GA and REINVENT. We also compare our approach with TextGrad [89], a recent work that similarly utilizes an LLM to make textual updates to SMILES strings. The key difference is that TextGrad’s improvement proposals are pointwise, conditioning only on the latest molecule, whereas Feedback Descent conditions on accumulated feedback history, enabling more effective continual improvement at high iteration budgets.

Main Results. Table 3 summarizes optimization outcomes across six protein targets. Feedback Descent outperforms all baselines and achieves the strongest scores on all targets. On multiple proteins, it matches or exceeds the 99.9th and even 99.99th percentiles of the DOCKSTRING database, including surpassing the best molecule present in the database itself ($N = 260155$). Notably, TextGrad consistently underperforms Feedback Descent across all targets; while the TextGrad paper evaluated on similar DOCKSTRING tasks for only ~ 10 iterations, we run both methods for 1000 steps and find that TextGrad’s pointwise conditioning does not scale well to high iteration budgets, confirming that accumulated feedback history is essential for sustained improvement. These findings show

Noise	ADRB1	PGR	PPARG
None	10.62	9.62	10.19
25%	9.28	9.14	8.16
50%	10.21	8.92	8.75
100%	6.60	8.39	6.78

Table 4: DOCKSTRING scores for ADRB1, PGR, and PPARG with Feedback Descent at varying feedback noise levels. **Performance degrades gracefully with increasing noise.**

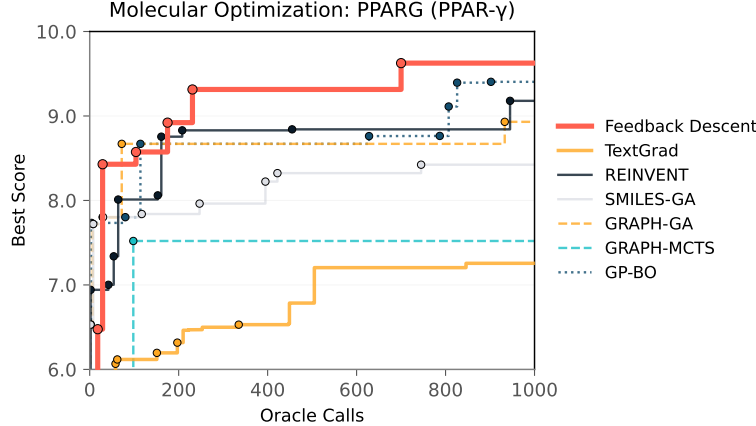


Figure 4: Optimization trajectories on PPARG showing docking scores over oracle calls for Feedback Descent and specialized baselines. **Feedback Descent quickly improves molecular docking scores within the first few hundred oracle calls.**

that Feedback Descent, a purely text-based method, can rival or outperform specialized graph-based algorithms, despite lacking handcrafted structural priors.

Figure 4 shows optimization trajectories for PPARG. Feedback Descent achieves competitive trajectories relative to specialized methods, reaching high-scoring regions of chemical space with comparable or fewer oracle calls. This pattern holds across targets, suggesting that the method generalizes rather than relying on idiosyncrasies of a single protein system.

Analysis of discovered molecules. Figure 5 illustrates the Pareto frontier between docking affinity (Vina score) and drug-likeness (QED) for PPARG. Feedback Descent recovers molecules that sit on or above the DOCKSTRING frontier, indicating that improvements in affinity are achieved without compromising drug-likeness. See Figure 7 in the appendix for the full set of Pareto frontiers across all targets. These results show that feedback-guided search yields candidates that are not only potent but also balanced along multiple drug-relevant dimensions.

We also examine novelty by plotting Tversky similarity (CFP4 fingerprints) to approved DrugBank molecules against docking scores in Figure 6. Across all targets, the correlations are weak or negative (Spearman ρ between -0.39 and 0.40), indicating that high-scoring candidates identified by Feedback Descent do not simply recycle functional groups from existing drugs, but instead explore novel regions of chemical space. For CDK2, no comparison is shown, as the target lacks any fully approved drugs in DrugBank with orthosteric binding as part of their mechanism of action, and thus does not satisfy our inclusion criteria.

Feedback quality and type. In addition to the main points of comparison, we show three ablations on the quality of the feedback in Table 3. We evaluate (1) **No Feedback**, i.e., parallel best-of-N sampling with no feedback; (2) **Random Feedback**, which uses the same iterative algorithm but shuffles rationales between molecule pairs; and (3) **Binary Only**, which provides only the binary signal of whether the newest molecule is better than the previous candidate. Random feedback underperforms even best-of-N, confirming that the method relies on feedback content rather than just the iterative structure. The gap between Binary Only and Feedback Descent (1.74 docking score units) demonstrates that textual rationales provide substantial value beyond the binary preference signal. Table 4 further tests robustness to corrupted feedback by randomly shuffling rationales at varying noise levels. The method degrades gracefully: 50% noise still achieves scores above the 99.9th percentile of DOCKSTRING for ADRB1 and PGR.

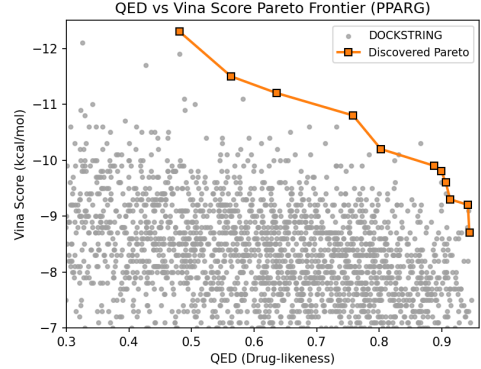


Figure 5: Pareto frontier of docking affinity vs. drug-likeness, comparing Feedback Descent molecules (blue) to the DOCKSTRING database (gray). **Feedback Descent finds novel molecules that meet or surpass known ones.**

Target	Win Rate
ADRB1	76%
CDK2	86%
F2	79%
PPARG	83%
Avg	81%

Table 5: True feedback vs. scrambled feedback win rate across 400 comparisons.

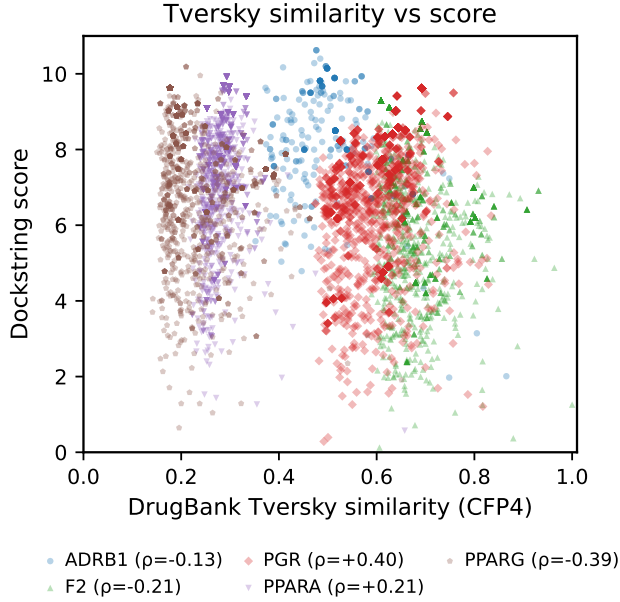


Figure 6: Scatter plots of Tversky similarity to approved drugs against docking scores, showing weak or negative correlations across targets. **High-scoring molecules discovered by Feedback Descent are far from any known drugs.**

Feedback alignment. Finally, we test whether generated molecules actually reflect the feedback shown during optimization in Table 5. We present an LLM judge with a newly generated molecule and ask it to determine whether the molecule more closely follows the true feedback or a scrambled control. We randomly flip the order shown to the judge to account for order bias. Across 400 comparisons, true feedback wins 81% of head-to-head comparisons ($p < 10^{-10}$, binomial test), demonstrating that the generator reliably reads and incorporates structured property feedback.

Feedback Descent Can Discover Novel Targeted Molecules

Feedback Descent, operating in a purely textual form, consistently identifies novel molecules that surpass high-percentile baselines in DOCKSTRING. This demonstrates that iterative, feedback-guided optimization can enable models to genuinely explore unknown design spaces beyond their training distribution.

5. Discussion

This paper presents Feedback Descent, an inference-time framework that improves text artifacts through structured pairwise feedback. We validate it on visual design, prompt optimization, and molecule discovery, showing that text can serve as an optimizable medium, not just static data. Unlike parameter tuning, this approach can leverage richer textual signals, allowing for continual improvement without requiring retraining.

Limitations. The method relies on strong evaluators, which may be scarce in some domains. Training models to produce reliable feedback remains a prerequisite for harder tasks. For creative domains, strictly “following the gradient” may be limiting; balancing refinement with exploration is an important next step.

Acknowledgments

We would like to thank Wanqiao Xu, Allen Nie, Henrik Marklund, Mert Yuksekgonul, Anikait Singh, and Jubayer Ibn Hamid for helpful discussions and feedback. This work is supported by the OpenAI Superalignment Fellowship, the KFAS Fellowship, and the Schmidt Sciences AI2050 program.

References

- [1] Alekh Agarwal, Peter L Bartlett, Pradeep Ravikumar, and Martin J Wainwright. Information-theoretic lower bounds on the oracle complexity of stochastic convex optimization. *IEEE Transactions on Information Theory*, 58(5):3235–3249, 2012.
- [2] Mayank Agarwal, Ibrahim Abdelaziz, Kinjal Basu, Merve Unuvar, Luis A Lastras, Yara Rizk, and Pavan Kapanipathi. Toolrm: Outcome reward models for tool-calling large language models. *arXiv preprint arXiv:2509.11963*, 2025.
- [3] Lakshya A Agrawal, Shangyin Tan, Dilara Soylu, Noah Ziems, Rishi Khare, Krista Opsahl-Ong, Arnav Singhvi, Herumb Shandilya, Michael J Ryan, Meng Jiang, et al. Gepa: Reflective prompt evolution can outperform reinforcement learning. *arXiv preprint arXiv:2507.19457*, 2025.
- [4] Jacob Austin, Augustus Odena, Maxwell I. Nye, Maarten Bosma, Henryk Michalewski, David Dohan, Ellen Jiang, Carrie J. Cai, Michael Terry, Quoc V. Le, and Charles Sutton. Program synthesis with large language models. *arXiv preprint arXiv:2108.07732*, 2021.
- [5] Mohammad Gheshlaghi Azar, Mark Rowland, Bilal Piot, Daniel Guo, Daniele Calandriello, Michal Valko, and Remi Munos. A general theoretical paradigm to understand learning from human preferences. *arXiv preprint arXiv:2310.12036*, 2023.
- [6] Yuntao Bai, Saurav Kadavath, Sandipan Kundu, Amanda Askell, Jackson Kernion, Andy Jones, Anna Chen, Anna Goldie, Azalia Mirhoseini, Cameron McKinnon, et al. Constitutional ai: Harmlessness from ai feedback. *arXiv preprint arXiv:2212.08073*, 2022.
- [7] Nathan Brown, Marco Fiscato, Marwin HS Segler, and Alain C Vaucher. Guacamol: Benchmarking models for de novo molecular design. *Journal of Chemical Information and Modeling*, 59(3):1096–1108, 2019. doi: 10.1021/acs.jcim.8b00839.
- [8] Sébastien Bubeck, Varun Chandrasekaran, Ronen Eldan, Johannes Gehrke, Eric Horvitz, Ece Kamar, Peter Lee, Yin Tat Lee, Yuanzhi Li, Scott Lundberg, et al. Sparks of artificial general intelligence: Early experiments with gpt-4. *arXiv preprint arXiv:2303.12712*, 2023.
- [9] Mark Chen, Jerry Tworek, Heewoo Jun, Qiming Yuan, Henrique Ponde de Oliveira Pinto, Jared Kaplan, Harri Edwards, Yura Burda, Nicholas Joseph, Greg Brockman, Alex Ray, Raul Puigdomenech, Alec Radford, Vedant Sastry, Ilya Sutskever, Daniel M. Ziegler, Amanda Dennison, Marius Ervin, William Perez, Sallaheddine Karaa, Sarah Kluska, Jerome Lespiau, Tom B. Brown, and David Wu. Evaluating large language models trained on code. *arXiv preprint arXiv:2107.03374*, 2021.
- [10] Xiangyi Chen, Sijia Liu, Kaidi Xu, Xingguo Li, Xue Lin, Mingyi Hong, and David Cox. Zo-adamm: Zeroth-order adaptive momentum method for black-box optimization. 2019.
- [11] Xiangyi Chen, Sijia Liu, and Mingyi Hong. Derivative-free optimization for low-rank adaptation in large language models. *arXiv preprint arXiv:2403.01754*, 2024.
- [12] Yuri Chervonyi, Trieu H Trinh, Miroslav Olšák, Xiaomeng Yang, Hoang Nguyen, Marcelo Menegali, Junehyuk Jung, Vikas Verma, Quoc V Le, and Thang Luong. Gold-medalist performance in solving olympiad geometry with alphageometry2. *arXiv preprint arXiv:2502.03544*, 2025. URL <https://arxiv.org/abs/2502.03544>.

[13] Paul F Christiano, Jan Leike, Tom Brown, Miljan Martic, Shane Legg, and Dario Amodei. Deep reinforcement learning from human preferences. *Advances in Neural Information Processing Systems*, 30, 2017.

[14] Hyung Won Chung, Le Hou, Shayne Longpre, Barret Zoph, Yi Tay, William Fedus, Eric Li, Xuezhe Wang, Mostafa Dehghani, Siddhartha Brahma, Albert Webson, Shixiang Shane Gu, Zhuyun Dai, Mirac Suzgun, Xinyun Chen, Aakanksha Chowdhery, Sharan Narang, Gaurav Mishra, Adams Yu, Vincent Zhao, Yanping Huang, Andrew Dai, Hongkun Yu, Slav Petrov, Ed H. Chi, Jeff Dean, Jacob Devlin, Adam Roberts, Denny Zhou, Quoc V. Le, and Jason Wei. Scaling instruction-finetuned language models. *arXiv preprint arXiv:2210.11416*, 2022.

[15] Karl Cobbe, Vineet Kosaraju, Mohammad Bavarian, Mark Chen, Heewoo Jun, Lukasz Kaiser, Matthias Plappert, Jerry Tworek, Jacob Hilton, Reiichiro Nakano, Christopher Hesse, and John Schulman. Training verifiers to solve math word problems. *arXiv preprint arXiv:2110.14168*, 2021.

[16] CodeGemma Team, Heri Zhao, et al. Codegemma: Open code models based on gemma. *arXiv preprint arXiv:2406.11409*, 2024.

[17] DeepSeek-AI, Daya Guo, Dejian Yang, Haowei Zhang, Junxiao Song, Ruoyu Zhang, Runxin Xu, Qihao Zhu, Shirong Ma, Peiyi Wang, et al. Deepseek-r1: Incentivizing reasoning capability in llms via reinforcement learning. *arXiv preprint arXiv:2501.12948*, 2025. URL <https://arxiv.org/abs/2501.12948>.

[18] Wanyu Du, Vipul Raheja, Dhruv Kumar, Zae Myung Kim, Melissa Lopez, and Dongyeop Kang. Read, revise, repeat: A system demonstration for human-in-the-loop iterative text revision. *In2Writing*, 2022.

[19] Kawin Ethayarajh, Winnie Xu, Niklas Muennighoff, Dan Jurafsky, and Douwe Kiela. Kto: Model alignment as prospect theoretic optimization. *arXiv preprint arXiv:2402.01306*, 2024.

[20] Xidong Feng, Bo Liu, Yan Song, Haotian Fu, Ziyu Wan, Girish A Koushik, Zhiyuan Hu, Mengyue Yang, Ying Wen, and Jun Wang. Natural language reinforcement learning. *arXiv preprint arXiv:2411.14251*, 2024.

[21] Wenhao Gao, Tianfan Fu, Jimeng Sun, and Connor W Coley. Sample efficiency matters: A benchmark for practical molecular optimization. *arXiv preprint arXiv:2206.12411*, 2022.

[22] Miguel García-Ortegón, Gregor N. C. Simm, Austin J. Tripp, José Miguel Hernández-Lobato, Matthias R. Bauer, and Sergio Bacallado. Dockstring: Easy molecular docking yields better benchmarks for ligand design. *Journal of Chemical Information and Modeling*, 62(15):3486–3502, 2022. doi: 10.1021/acs.jcim.1c01334.

[23] Anna Gaulton, Louisa J Bellis, A Patricia Bento, Jon Chambers, Mark Davies, Anne Hersey, Yvonne Light, Shaun McGlinchey, David Michalovich, Bissan Al-Lazikani, and John P Overington. Chemb: a large-scale bioactivity database for drug discovery. *Nucleic Acids Research*, 40(D1):D1100–D1107, 2012. doi: 10.1093/nar/gkr777.

[24] Jonas Geiping, Sean McLeish, Neel Jain, John Kirchenbauer, Siddharth Singh, Brian R Bartoldson, Bhavya Kailkhura, Abhinav Bhatele, and Tom Goldstein. Scaling up test-time compute with latent reasoning: A recurrent depth approach. *arXiv preprint arXiv:2502.05171*, 2025.

[25] Michael K Gilson, Tiqing Liu, Michael Baitaluk, George Nicola, Linda Hwang, and Justin Chong. Bindingdb in 2015: a public database for medicinal chemistry, computational chemistry and systems pharmacology. *Nucleic Acids Research*, 44(D1):D1045–D1053, 2016. doi: 10.1093/nar/gkv1072.

[26] David E Golberg. Genetic algorithms in search, optimization, and machine learning. *Addion wesley*, 1989 (102):36, 1989.

[27] Daya Guo, Qihao Zhu, Dejian Yang, Zhenda Xie, Kai Dong, Wentao Zhang, Guanting Chen, Xiao Bi, Yu Wu, YK Li, et al. Deepseek-coder: When the large language model meets programming – the rise of code intelligence. *arXiv preprint arXiv:2401.14196*, 2024.

[28] Zerui Guo, Tianxiang Sun, Xipeng Qiu, and Xuanjing Huang. When gradient descent meets derivative-free optimization: A match made in black-box scenario. *arXiv preprint arXiv:2305.10013*, 2023.

[29] John H Holland. *Adaptation in natural and artificial systems: an introductory analysis with applications to biology, control, and artificial intelligence*. MIT press, 1992.

[30] Jan H Jensen. A graph-based genetic algorithm and generative model/monte carlo tree search for the exploration of chemical space. *Chemical Science*, 10(12):3567–3572, 2019. doi: 10.1039/C8SC05372C.

[31] Yichen Jiang, Shikha Bordia, Zheng Zhong, Charles Dognin, Maneesh Singh, and Mohit Bansal. Hover: A dataset for many-hop fact extraction and claim verification. In *Findings of the Association for Computational Linguistics: EMNLP 2020*, pages 3441–3460, 2020. doi: 10.18653/v1/2020.findings-emnlp.309.

[32] Hoang Anh Just, Ming Jin, Anit Sahu, Huy Phan, and Ruoxi Jia. Data-centric human preference optimization with rationales. *arXiv preprint arXiv:2407.14477*, 2024.

[33] Omar Khattab, Keshav Santhanam, Xiang Lisa Li, David Hall, Percy Liang, Christopher Potts, and Matei Zaharia. Demonstrate-search-predict: Composing retrieval and language models for knowledge-intensive nlp. *arXiv preprint arXiv:2212.14024*, 2022.

[34] Omar Khattab, Arnav Singhvi, Paridhi Maheshwari, Zhiyuan Zhang, Keshav Santhanam, Sri Vardhamanan, Saiful Haq, Ashutosh Sharma, Thomas T Joshi, Hanna Moazam, Heather Miller, Matei Zaharia, and Christopher Potts. Dspy: Compiling declarative language model calls into self-improving pipelines. *arXiv preprint arXiv:2310.03714*, 2024.

[35] Andrew K Lampinen, Nicholas Roy, Ishita Dasgupta, Stephanie Cy Chan, Allison Tam, James McClelland, Chen Yan, Adam Santoro, Neil C Rabinowitz, Jane Wang, and Felix Hill. Tell me why! Explanations support learning relational and causal structure. In *Proceedings of the 39th International Conference on Machine Learning*, volume 162 of *Proceedings of Machine Learning Research*, pages 11868–11890. PMLR, 2022.

[36] Greg Landrum. Rdkit: Open-source cheminformatics, 2006. URL <http://www.rdkit.org>.

[37] Robert Tjarko Lange, Yingtao Tian, and Yujin Tang. Large language model-based evolutionary optimizer: Reasoning with elitism. *arXiv preprint arXiv:2403.02054*, 2024.

[38] Siyan Li, Vethavikashini Chithrra Raghuram, Omar Khattab, Julia Hirschberg, and Zhou Yu. Papillon: Privacy preservation from internet-based and local language model ensembles. In *Proceedings of the 2025 Conference of the North American Chapter of the Association for Computational Linguistics*, 2025. NAACL 2025.

[39] Tiqing Liu, Yuhmei Lin, Xin Wen, Robert N Jorissen, and Michael K Gilson. Bindingdb: a web-accessible database of experimentally determined protein–ligand binding affinities. *Nucleic Acids Research*, 35(suppl_1):D198–D201, 2007. doi: 10.1093/nar/gkl999.

[40] Shayne Longpre, Le Hou, Tu Vu, Albert Webson, Hyung Won Chung, Yi Tay, Denny Zhou, Quoc V. Le, Barret Zoph, Jason Wei, and Adam Roberts. The flan collection: Designing data and methods for effective instruction tuning. *ICML*, 2023.

[41] Anton Lozhkov, Raymond Li, Loubna Ben Allal, Denis Kocetkov, Chenghao Mou, Christopher Akiki, Carlos Muñoz Ferrandis, Muennighoff Niklas, Jean Kaddour, Yacine Jernite, et al. Starcoder 2 and the stack v2: The next generation. *arXiv preprint arXiv:2402.19173*, 2024.

[42] Aman Madaan, Niket Tandon, Prakhar Gupta, Skyler Hallinan, Luyu Gao, Sarah Wiegreffe, Uri Alon, Nouha Dziri, Shrimai Prabhumoye, Yiming Yang, Sean Welleck, Bodhisattwa Prasad Majumder, Shashank Gupta, Amir Yazdanbakhsh, and Peter Clark. Self-refine: Iterative refinement with self-feedback. *arXiv preprint arXiv:2303.17651*, 2023.

[43] David Mendez, Anna Gaulton, A Patrícia Bento, Jon Chambers, Marleen De Veij, Eloy Félix, María Paula Magariños, José F Mosquera, Prudence Mutowo, Michał Nowotka, et al. Chemb1: towards direct deposition of bioassay data. *Nucleic Acids Research*, 47(D1):D930–D940, 2019. doi: 10.1093/nar/gky1075.

[44] Swaroop Mishra and Elnaz Nouri. Help me think: A simple prompting strategy for non-experts to create customized content with models. pages 11834–11890, 2023.

[45] Niklas Muennighoff, Zitong Yang, Weijia Shi, Xiang Lisa Li, Li Fei-Fei, Hannaneh Hajishirzi, Luke Zettlemoyer, Percy Liang, Emmanuel Candès, and Tatsunori B Hashimoto. s1: Simple test-time scaling. *arXiv preprint arXiv:2501.19393*, 2025.

[46] Remi Munos, Michal Valko, Daniele Calandriello, Mohammad Gheshlaghi Azar, Mark Rowland, Zhao-han Daniel Guo, Yunhao Tang, Matthieu Geist, Thomas Mesnard, Côme Fiege1, Andrea Michi, Marco Selvi, Sertan Girgin, Nikola Momchev, Olivier Bachem, Daniel J Mankowitz, Doina Precup, and Bilal Piot. Nash learning from human feedback. In *Proceedings of the 41st International Conference on Machine Learning*, volume 235 of *Proceedings of Machine Learning Research*, pages 36743–36768. PMLR, 2024.

[47] Arkadi S Nemirovski and David Borisovich Yudin. *Problem Complexity and Method Efficiency in Optimization*. Wiley-Interscience, New York, 1983.

[48] Yurii Nesterov and Vladimir Spokoiny. Random gradient-free minimization of convex functions. *Foundations of Computational Mathematics*, 17(2):527–566, 2017. doi: 10.1007/s10208-015-9296-2.

[49] Allen Nie, Ching-An Cheng, Andrey Kolobov, and Adith Swaminathan. The importance of directional feedback for llm-based optimizers. *arXiv preprint arXiv:2405.16434*, 2024.

[50] Erik Nijkamp, Bo Pang, Hiroaki Hayashi, Lifu Tu, Huan Wang, Yingbo Zhou, Silvio Savarese, and Caiming Xiong. Codegen: An open large language model for code with multi-turn program synthesis. *arXiv preprint arXiv:2203.13474*, 2022.

[51] Marcus Olivecrona, Thomas Blaschke, Ola Engkvist, and Hongming Chen. Molecular de novo design through deep reinforcement learning. *Journal of Cheminformatics*, 9(1):1–14, 2017. doi: 10.1186/s13321-017-0235-x.

[52] OpenAI. Openai o1 system card. Technical report, OpenAI, 2024. URL <https://arxiv.org/abs/2412.16720>.

[53] Krista Opsahl-Ong, Michael J Ryan, Josh Purtell, David Broman, Christopher Potts, Matei Zaharia, and Omar Khattab. Optimizing instructions and demonstrations for multi-stage language model programs. *arXiv preprint arXiv:2406.11695*, 2024.

[54] Long Ouyang, Jeffrey Wu, Xu Jiang, Diogo Almeida, Carroll Wainwright, Pamela Mishkin, Chong Zhang, Sandhini Agarwal, Katarina Slama, Alex Ray, John Schulman, Jacob Hilton, Fraser Kelton, Luke Miller, Maddie Simens, Amanda Askell, Peter Welinder, Paul F Christiano, Jan Leike, and Ryan Lowe. Training language models to follow instructions with human feedback. *Advances in Neural Information Processing Systems*, 35:27730–27744, 2022.

[55] Aaron Parisi, Yao Zhao, and Noah Fiedel. Talm: Tool augmented language models. *arXiv preprint arXiv:2205.12255*, 2022.

[56] Reid Pryzant, Dan Iter, Jerry Li, Yin Tat Lee, Chenguang Zhu, and Michael Zeng. Automatic prompt optimization with “gradient descent” and beam search. *arXiv preprint arXiv:2305.03495*, 2023.

[57] Valentina Pyatkin, Saumya Malik, Victoria Graf, Hamish Ivison, Shengyi Huang, Pradeep Dasigi, Nathan Lambert, and Hannaneh Hajishirzi. Generalizing verifiable instruction following. *arXiv preprint arXiv:2507.02833*, 2025.

[58] Yujia Qin, Shengding Hu, Yankai Lin, Weize Chen, Ning Ding, Ganqu Cui, Zheni Zeng, Yufei Huang, Chaojun Xiao, Chi Han, Yi Ren Fung, Yusheng Su, Huadong Wang, Cheng Qian, Runchu Tian, Kunlun Zhu, Shihao Liang, Xingyu Shen, Bokai Xu, Zhen Zhang, Yining Ye, Bowen Li, Ziwei Tang, Jing Yi, Yuzhang Zhu, Zhenning Dai, Lan Yan, Xin Cong, Yaxi Lu, Weilin Zhao, Yuxiang Huang, Junxi Yan, Xu Han, Xian Sun, Dahai Li, Jason Phang, Cheng Yang, Tongshuang Wu, Heng Ji, Zhiyuan Liu, and Maosong Sun. Tool learning with foundation models. *arXiv preprint arXiv:2304.08354*, 2023.

[59] Rafael Rafailov, Archit Sharma, Eric Mitchell, Stefano Ermon, Christopher D Manning, and Chelsea Finn. Direct preference optimization: Your language model is secretly a reward model. *arXiv preprint arXiv:2305.18290*, 2023.

[60] Baptiste Roziere, Jonas Gehring, Fabian Gloeckle, Sten Sootla, Itai Gat, Xiaoqing Ellen Tan, Yossi Adi, Jingyu Liu, Tal Remez, Jérémie Rapin, Artyom Kozhevnikov, Ivan Evtimov, Joanna Bitton, Manish Bhatt, Cristian Canton Ferrer, Aaron Grattafiori, Wenhan Xiong, Alexandre Défossez, Jade Copet, Faisal Azhar, Hugo Touvron, Louis Martin, Nicolas Usunier, Thomas Scialom, and Gabriel Synnaeve. Code llama: Open foundation models for code. *arXiv preprint arXiv:2308.12950*, 2023.

[61] William Saunders, Catherine Yeh, Jeff Wu, Steven Bills, Long Ouyang, Jonathan Ward, and Jan Leike. Self-critiquing models for assisting human evaluators. *arXiv preprint arXiv:2206.05802*, 2022.

[62] Jérémie Scheurer, Jon Ander Campos, Jun Shern Chan, Angelica Chen, Kyunghyun Cho, and Ethan Perez. Training language models with language feedback at scale. *arXiv preprint arXiv:2303.16755*, 2023.

[63] Timo Schick, Jane Dwivedi-Yu, Zhengbao Jiang, Fabio Petroni, Patrick Lewis, Gautier Izacard, Qingfei You, Christoforos Nalmpantis, Edouard Grave, and Sebastian Riedel. Peer: A collaborative language model. *arXiv preprint arXiv:2208.11663*, 2022.

[64] Timo Schick, Jane Dwivedi-Yu, Roberto Densi, Roberta Raileanu, Maria Lomeli, Luke Zettlemoyer, Nicola Cancedda, and Thomas Scialom. Toolformer: Language models can teach themselves to use tools. *NeurIPS*, 2023.

[65] Zhihong Shao, Peiyi Wang, Qihao Zhu, Runxin Xu, Junxiao Song, Xiao Bi, Haowei Zhang, Mingchuan Zhang, YK Li, Yang Wu, et al. Deepseekmath: Pushing the limits of mathematical reasoning in open language models. *arXiv preprint arXiv:2402.03300*, 2024.

[66] David Silver and Richard S. Sutton. Welcome to the era of experience. In *Designing an Intelligence*. MIT Press, 2025. Preprint.

[67] Charlie Snell, Jaehoon Lee, Kelvin Xu, and Aviral Kumar. Scaling llm test-time compute optimally can be more effective than scaling model parameters. *arXiv preprint arXiv:2408.03314*, 2024.

[68] Tianxiang Sun, Zhengfu Chen, Xipeng Qiu, and Xuanjing Huang. Bbtv2: Towards a gradient-free future with large language models. *arXiv preprint arXiv:2205.11200*, 2022.

[69] The UniProt Consortium. Uniprot: the universal protein knowledgebase in 2023. *Nucleic Acids Research*, 51(D1):D523–D531, 2023. doi: 10.1093/nar/gkac1052.

[70] Austin Tripp, Gregor N. C. Simm, and José Miguel Hernández-Lobato. A fresh look at de novo molecular design benchmarks. In *NeurIPS 2021 AI for Science Workshop*, 2021. URL https://openreview.net/forum?id=gS3XMun4c1_.

[71] Haorui Wang, Marta Skreta, Cher-Tian Ser, Wenhao Gao, Lingkai Kong, Felix Strieth-Kalthoff, Chenru Duan, Yuchen Zhuang, Yue Yu, Yanqiao Zhu, et al. Efficient evolutionary search over chemical space with large language models. *arXiv preprint arXiv:2406.16976*, 2024.

[72] Jiayi Wang, Yuxuan Sun, Wenjia Zhang, et al. Adaptive preference scaling for reinforcement learning with human feedback. *arXiv preprint arXiv:2406.02764*, 2024.

[73] Lei Wang, Chen Ma, Xueyang Feng, Zeyu Zhang, Hao Yang, Jingsen Zhang, Zhiyuan Chen, Jiakai Tang, Xu Chen, Yankai Lin, et al. A survey on large language model based autonomous agents. *arXiv preprint arXiv:2308.11432*, 2023.

[74] Yue Wang, Hung Le, Akhilesh Deepmare, Nghi D.Q. Bui, Junnan Li, and Steven C.H. Hoi. Codet5+: Open code large language models for code understanding and generation. *Proceedings of EMNLP*, 2023.

[75] Jason Wei, Maarten Bosma, Vincent Y. Zhao, Kelvin Guu, Adams Wei Yu, Brian Lester, Nan Du, Andrew M. Dai, and Quoc V. Le. Finetuned language models are zero-shot learners. *ICLR*, 2022.

[76] Jason Wei, Xuezhi Wang, Dale Schuurmans, Maarten Bosma, Brian Ichter, Fei Xia, Ed H. Chi, Quoc V. Le, and Denny Zhou. Chain-of-thought prompting elicits reasoning in large language models. In *NeurIPS*, 2022.

[77] David Weininger. Smiles, a chemical language and information system. 1. introduction to methodology and encoding rules. *Journal of Chemical Information and Computer Sciences*, 28(1):31–36, 1988. doi: 10.1021/ci00057a005.

[78] Sean Welleck, Ximing Lu, Peter West, Faeze Brahman, Tianxiao Shen, Daniel Khashabi, and Yejin Choi. Generating sequences by learning to self-correct. *ICLR*, 2023.

[79] Christian Wirth, Riad Akroud, Gerhard Neumann, and Johannes Fürnkranz. A survey of preference-based reinforcement learning methods. *Journal of Machine Learning Research*, 18(136):1–46, 2017.

[80] Zeqiu Wu, Yushi Hu, Weijia Shi, Nouha Dziri, Alane Suhr, Prithviraj Ammanabrolu, Noah A. Smith, Mari Ostendorf, and Hannaneh Hajishirzi. Fine-grained human feedback gives better rewards for language model training. *arXiv preprint arXiv:2306.01693*, 2023.

[81] Wei Xiong, Hanze Dong, Chenlu Ye, Han Zhong, Nan Jiang, and Tong Zhang. Iterative preference learning from human feedback: Bridging theory and practice for rlhf under kl-constraint. *arXiv preprint arXiv:2312.11456*, 2023.

[82] An Yang, Anfeng Li, Baosong Yang, Beichen Zhang, Binyuan Hui, Bo Zheng, Bowen Yu, Chang Gao, Chengan Huang, Chenxu Lv, et al. Qwen3 technical report. *arXiv preprint arXiv:2505.09388*, 2025.

[83] Chengrun Yang, Xuezhi Wang, Yifeng Lu, Hanxiao Liu, Quoc V. Le, Denny Zhou, and Xinyun Chen. Large language models as optimizers. *arXiv preprint arXiv:2309.03409*, 2023.

[84] Wenkai Yang, Shuming Ma, Yankai Lin, and Furu Wei. Towards thinking-optimal scaling of test-time compute for llm reasoning. *arXiv preprint arXiv:2502.18080*, 2025.

[85] Zhilin Yang, Peng Qi, Saizheng Zhang, Yoshua Bengio, William Cohen, Ruslan Salakhutdinov, and Christopher D. Manning. Hotpotqa: A dataset for diverse, explainable multi-hop question answering. In *Proceedings of the 2018 Conference on Empirical Methods in Natural Language Processing*, pages 2369–2380. Association for Computational Linguistics, 2018.

[86] Shunyu Yao, Dian Yu, Jeffrey Zhao, Izhak Shafran, Thomas L. Griffiths, Yuan Cao, and Karthik Narasimhan. Tree of Thoughts: Deliberate problem solving with large language models. 2023.

[87] Shunyu Yao, Jeffrey Zhao, Dian Yu, Nan Du, Izhak Shafran, Karthik Narasimhan, and Yuan Cao. React: Synergizing reasoning and acting in language models. *ICLR*, 2023.

[88] Yue Yu, Zhengxing Chen, Aston Zhang, Liang Tan, Chenguang Zhu, Richard Yuanzhe Pang, Yundi Qian, Xuewei Wang, Suchin Gururangan, Chao Zhang, et al. Self-generated critiques boost reward modeling for language models. *arXiv preprint arXiv:2411.16646*, 2024.

[89] Mert Yuksekgonul, Federico Bianchi, Joseph Boen, Sheng Liu, Pan Lu, Zhi Huang, Carlos Guestrin, and James Zou. Textgrad: Automatic "differentiation" via text. *arXiv preprint arXiv:2406.07496*, 2024.

- [90] Eric Zelikman, Yuhuai Wu, Jesse Mu, and Noah D. Goodman. Star: Bootstrapping reasoning with reasoning. *arXiv preprint arXiv:2203.14465*, 2022.
- [91] Shengyu Zhang, Linfeng Dong, Xiaoya Li, Sen Zhang, Xiaofei Sun, Shuhe Wang, Jiwei Li, Runyi Hu, Tianwei Zhang, Fei Wu, et al. Instruction tuning for large language models: A survey. *arXiv preprint arXiv:2308.10792*, 2024.
- [92] Yongchao Zhou, Andrei Ioan Muresanu, Ziwen Han, Keiran Paster, Silviu Pitis, Harris Chan, and Jimmy Ba. Large language models are human-level prompt engineers. *arXiv preprint arXiv:2211.01910*, 2022.
- [93] Qihao Zhu, Daya Guo, Zhihong Shao, Dejian Yang, Peiyi Wang, Runxin Xu, Y Wu, Yukun Li, Huazuo Gao, Shirong Ma, et al. Deepseek-coder-v2: Breaking the barrier of closed-source models in code intelligence. *arXiv preprint arXiv:2406.11931*, 2024.

A. Formal Statements and Proofs

Proposition 1 (Linear convergence under PL with rationale-guided directions). *Let $r : Z \rightarrow \mathbb{R}$ be L -smooth and satisfy the μ -PL condition (for maximization)*

$$\frac{1}{2} \|\nabla r(z)\|_2^2 \geq \mu(r(z^*) - r(z)) \quad \forall z \in Z.$$

At iteration t , suppose a direction v_t satisfies

$$\mathbb{E}[v_t | z_t] = \alpha \nabla r(z_t), \quad \mathbb{E}[\|v_t - \mathbb{E}[v_t | z_t]\|_2^2 | z_t] \leq \sigma^2 \|\nabla r(z_t)\|_2^2,$$

with constants $\alpha > 0$ and $\sigma \geq 0$, and define $\kappa_1 \triangleq \alpha^2 + \sigma^2$. Consider the update $z_{t+1} = z_t + \eta v_t$. If a constraint set Z is present, assume $z_t + \eta v_t \in Z$ (i.e., the projection is inactive). With stepsize $\eta = \alpha/(L\kappa_1)$,

$$\mathbb{E}[r(z^*) - r(z_{t+1}) | z_t] \leq \left(1 - \frac{\mu\alpha^2}{L\kappa_1}\right) [r(z^*) - r(z_t)].$$

Unrolling yields

$$\mathbb{E}[r(z^*) - r(z_T)] \leq \left(1 - \frac{\mu\alpha^2}{L\kappa_1}\right)^T [r(z^*) - r(z_0)],$$

so ϵ -accuracy is achieved in

$$T = O\left(\frac{L(\alpha^2 + \sigma^2)}{\mu\alpha^2} \log \frac{1}{\epsilon}\right)$$

iterations.

Proof. L -smoothness gives the two-sided bound

$$r(z_t + \eta v_t) \geq r(z_t) + \eta \langle \nabla r(z_t), v_t \rangle - \frac{L}{2} \eta^2 \|v_t\|_2^2.$$

Taking conditional expectation and using $\mathbb{E}[v_t | z_t] = \alpha \nabla r(z_t)$ and $\mathbb{E}[\|v_t\|_2^2 | z_t] \leq (\alpha^2 + \sigma^2) \|\nabla r(z_t)\|_2^2 = \kappa_1 \|\nabla r(z_t)\|_2^2$,

$$\mathbb{E}[r(z_{t+1}) | z_t] \geq r(z_t) + \left(\eta\alpha - \frac{L}{2}\eta^2\kappa_1\right) \|\nabla r(z_t)\|_2^2.$$

By the PL inequality, $\|\nabla r(z_t)\|_2^2 \geq 2\mu[r(z^*) - r(z_t)]$, so

$$\mathbb{E}[r(z^*) - r(z_{t+1}) | z_t] \leq \left(1 - 2\mu\eta\alpha + \mu L\eta^2\kappa_1\right) [r(z^*) - r(z_t)].$$

Choosing $\eta = \alpha/(L\kappa_1)$ makes the bracket equal to $1 - \mu\alpha^2/(L\kappa_1)$, yielding the claim. \square

A.1. Query Complexity and Dimension Dependence

Dimension-Free Case. When rationales provide full gradient information ($v_t \in \mathbb{R}^d$) at unit cost, the query complexity equals T and is dimension-independent:

$$\text{Queries} = O\left(\frac{L(\alpha^2 + \sigma^2)}{\alpha^2\mu} \log \frac{1}{\epsilon}\right) \tag{3}$$

Coordinate-Sparse Case. Suppose each query reveals one coordinate of $\nabla r(z_t)$ chosen uniformly at random. Using the unbiased estimator $v_t = d(\partial_i r(z_t)) e_i$ with $i \sim \text{Unif}([d])$ gives $\alpha = 1$, $\sigma^2 = d - 1$, and hence $\kappa_1 = d$ and stepsize $\eta = 1/(Ld)$. We have

$$T = O\left(\frac{Ld}{\mu} \log \frac{1}{\epsilon}\right), \quad \text{Queries} = O\left(\frac{Ld}{\mu} \log \frac{1}{\epsilon}\right).$$

Equivalently, averaging m independent coordinate queries per iteration yields $\sigma^2 = (d - 1)/m$; taking $m = d$ recovers $T = O((L/\mu) \log(1/\epsilon))$ with d queries per iteration, so total queries remain $\Theta(\frac{Ld}{\mu} \log \frac{1}{\epsilon})$.

This clarifies when and why dimension appears in the complexity.

B. Lower Bounds for Exhaustive/Random Zeroth-Order Search

We formalize the intrinsic slowness of exhaustive (grid) search and best-of- N random sampling when only function values (or preferences) are used without directional information. The hard instance is the strongly concave quadratic

$$r(z) = r(z^*) - \frac{\mu}{2} \|z - z^*\|_2^2, \quad z \in B_R(z^*) \subset \mathbb{R}^d,$$

whose ϵ -optimal set is the ball $B_{\rho_\epsilon}(z^*)$ with radius $\rho_\epsilon = \sqrt{2\epsilon/\mu}$.

Proposition 2 (Grid-search lower bound). *Let $B_R(z^*) \subset \mathbb{R}^d$ and a hypercubic grid of spacing h . Its covering radius is $\rho = \frac{\sqrt{d}h}{2}$. To guarantee that for all placements of z^* there exists a grid point in the ϵ -optimal ball $B_{\rho_\epsilon}(z^*)$ with $\rho_\epsilon = \sqrt{2\epsilon/\mu}$, it suffices that $\rho \leq \rho_\epsilon$ (i.e., $h \leq 2\rho_\epsilon/\sqrt{d}$). Furthermore, any such grid restricted to $B_R(z^*)$ must contain at least*

$$N \geq \left(\frac{R}{\rho}\right)^d = \left(\frac{R\sqrt{d}}{2\rho_\epsilon}\right)^d = \left(\frac{\mu R^2 d}{8\epsilon}\right)^{d/2}$$

points. Hence exhaustive grid search is exponential in d and polynomial in $1/\epsilon$ with exponent $d/2$ on this family.

Proof. Coverage of $B_R(z^*)$ by N balls of radius ρ centered at grid points implies $NV_d\rho^d \geq V_dR^d$, hence $N \geq (R/\rho)^d$. With $\rho = \sqrt{d}h/2$ and $h \leq 2\rho_\epsilon/\sqrt{d}$, we obtain $N \geq (R\sqrt{d}/(2\rho_\epsilon))^d$. Substitute $\rho_\epsilon = \sqrt{2\epsilon/\mu}$ to conclude. \square

Proposition 3 (Best-of- N random sampling lower bound). *Draw $X_1, \dots, X_N \stackrel{i.i.d.}{\sim} \text{Unif}(B_R(z^*))$ and let $\hat{z} = \arg \max_i r(X_i)$ for $r(z) = r(z^*) - \frac{\mu}{2}\|z - z^*\|_2^2$. Then with $a \triangleq 2/d$,*

$$\mathbb{E}[r(z^*) - r(\hat{z})] = \frac{\mu R^2}{2} N \text{B}(1+a, N) = \frac{\mu R^2}{2} \Gamma(1+a) \frac{\Gamma(N+1)}{\Gamma(N+1+a)}.$$

Moreover, for all $d \geq 1$ (so $a \in (0, 2]$),

$$\frac{\Gamma(N+1)}{\Gamma(N+1+a)} \geq (N+2)^{-a},$$

and thus

$$\mathbb{E}[r(z^*) - r(\hat{z})] \geq \frac{\mu R^2}{2} \Gamma\left(1 + \frac{2}{d}\right) (N+2)^{-\frac{2}{d}} = \Omega(N^{-\frac{2}{d}}).$$

Proof. Let $R_i = \|X_i - z^*\|_2$ and $R_{\min} = \min_i R_i$. The CDF of R_{\min} is $F(r) = 1 - (1 - (r/R)^d)^N$ for $r \in [0, R]$. Differentiating, $f(r) = Ndr^{d-1}R^{-d}(1 - (r/R)^d)^{N-1}$. Then

$$\mathbb{E}[R_{\min}^2] = \int_0^R r^2 f(r) dr = NR^2 \int_0^1 t^{\frac{2}{d}} (1-t)^{N-1} dt = NR^2 \text{B}\left(1 + \frac{2}{d}, N\right),$$

where $t = (r/R)^d$ and B is the Beta function. Using $\text{B}(a, b) = \frac{\Gamma(a)\Gamma(b)}{\Gamma(a+b)}$ gives the exact expression. For the bound, we use the inequality $\Gamma(N+1)/\Gamma(N+1+a) \geq (N+2)^{-a}$ which holds for all $a \in (0, 2]$ and $N \geq 1$. \square

C. Extended Experiment Section

C.1. Implementation Details

SVG Code Optimization. We employ a tournament-style approach where gpt-5-mini generates SVG/TikZ code that gets rendered to PNG images for pairwise aesthetic comparisons by a separate instance of the same model acting as judge. The system maintains a “champion” design that only updates when both A-vs-B and B-vs-A orderings consistently agree on a winner, accumulating winning rationales into the generation prompt to guide aesthetic improvements across iterations. The judge provides natural language rationales explaining aesthetic preferences that inform subsequent generations.

IFBench Prompt Optimization. We closely follow the setting of Agrawal et al. [3] for this experiment, including their choice of LLMs (Qwen3-8B and GPT-4.1-mini) and multi-stage DSPy programs. For Qwen3-8B, we use 10 iterations with no early stopping (patience=0) with temperature 0.6, and evaluate 2 prompt candidates per round across 20 hard examples. For GPT-4.1-mini, we increase to 15 iterations with early stopping (patience=5) with temperature 1.0 for exploration. Both configurations use the same prompt improver template, described in Section C.3.

We programmatically generate a textual description of the difference between two prompts. To compare two prompts, we first partition the training set into four quadrants based on outcomes: examples where prompt A succeeds and B fails (A_wins), A fails and B succeeds (B_wins), both fail (tie_fail), or both succeed (tie_success). We then use the same LLM to propose hypotheses about input characteristics (based on the prompt text) and output patterns (based on the response and evaluation feedback), producing around 20 hypotheses for each category. To evaluate whether each hypothesis applies to each example, we use the same LLM as the tagger that outputs binary labels (1 if the hypothesis matches, 0 otherwise) for all hypotheses in a single call per example, processing hundreds of examples in parallel. We then compute lift metrics for each hypothesis-quadrant pair, where lift is the ratio of conditional probability to the base rate (i.e., how much more likely an outcome is given the hypothesis holds). We validate the hypotheses statistically using Fisher’s exact test, and filter for hypotheses that are statistically significant at $p < 0.1$ with minimum support of 3 examples and lift ≥ 2.0 for A/B wins or ≥ 1.5 for failures. This analysis identifies which input patterns correlate with differential performance and which output characteristics appear when one prompt outperforms the other, providing actionable insights for prompt improvement.

Molecule Optimization. We implement molecular optimization using the DOCKSTRING package [22] for protein-ligand docking simulations across six therapeutic targets. The system begins with three simple seed molecules (acetamide, pentane, benzene) and progressively evolves SMILES strings through iterative feedback loops that incorporate RDKit molecular properties, protein binding site information, and similarity comparisons to approved drugs as metadata. We use the combined score function suggested by DOCKSTRING:

$$s_{\text{overall}}(\text{molecule}, \text{protein}) = -\text{Vina}(\text{molecule}, \text{protein}) - 10 * (1 - \text{QED}(\text{molecule})), \quad (4)$$

where Vina provides the binding affinity prediction (kcal/mol, more negative is better) and the QED penalty term penalizes molecules with poor drug-likeness, with lower overall scores indicating better molecules that balance binding strength and drug-like properties. Note that QED scores range from 0 to 1 while Vina scores typically range from -3.0 to -12.0 kcal/mol. For Feedback Descent, we use a batch size of 8 and top-k selection of 10 examples.

C.2. Additional Results

Figure 7 shows that across all protein targets, the discovered molecules extend beyond the DOCKSTRING baseline along both axes. The resulting Pareto frontiers illustrate consistent improvements in the joint trade-off between docking affinity and drug-likeness, highlighting that feedback-guided search yields coordinated gains rather than isolated outliers.

C.3. Prompt Templates

We use the following prompt for the judge for the Anatomy SVG task. The rubrics for the other tasks are written in a similar style, translating a particular aesthetic into operational rules that minimize ambiguity.

Anatomy Judge Rubric
RUBRIC NAME: Anatomical Realism

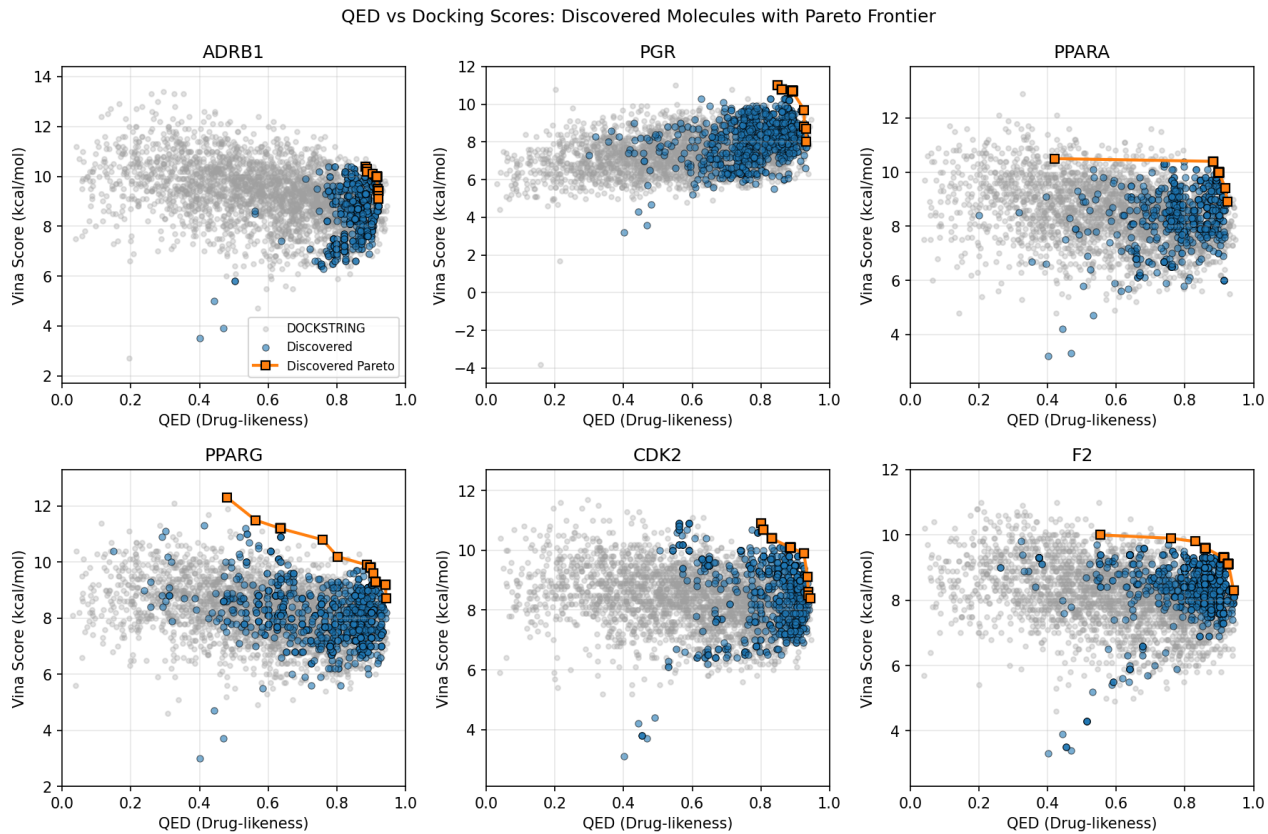


Figure 7: Pareto frontiers of discovered molecules (blue) compared against molecules in the DOCKSTRING dataset (gray) across six protein targets. The highlighted orange markers indicate molecules on the discovered Pareto frontier, achieving joint improvements in docking affinity (Vina score) and drug-likeness (QED).

INTENT: Believable equine anatomy with a plausible horn; form, proportion, and structure matter most.

NON-NEGOTIABLES:

- Recognizable equine proportions; head, neck, torso, four legs, mane, tail, horn present
- .
- Limbs connect anatomically; joints and hooves indicated.

CRITICAL BENCHMARKS (must evaluate these first):

1. Head-Neck Proportion: Neck length should be ~1.5x head length; head meets neck high on shoulders
2. Body Square: Body length (shoulder to buttock) ~ = height at withers; chest depth ~ = elbow height
3. Leg Structure: Proper joint articulation with elbow under withers; fetlock/pastern angles 45-55 deg when standing; all four limbs distinct and correctly connected

WHAT TO REWARD:

- Correct limb count and articulation; mass distribution that could stand or move.
- Horn integrates naturally with the skull (frontal bone center, 2-3" above eye line).
- Subtle shading or line variation conveying volume.

Method	ADRB1	PGR	PPARA	PPARG	CDK2	F2
DOCKSTRING (N=260155)	Top 50%	5.305	3.478	4.549	4.210	4.385
	Top 90%	8.785	7.878	7.987	7.658	7.733
	Top 99%	9.620	8.703	8.718	8.449	8.453
	Top 99.9%	10.209	9.260	9.230	9.012	8.979
	Top 99.99%	<u>10.742</u>	<u>9.723</u>	9.821	9.518	9.509
	Best Molecule	<u>11.330</u>	<u>9.742</u>	9.907	9.529	<u>9.311</u>
GP-BO [†] [70]	10.552 ± 0.140	9.307 ± 0.177	9.680 ± 0.337	9.485 ± 0.279	9.067 ± 0.289	8.686 ± 0.068
Graph MCTS [†] [30]	8.883 ± 0.826	7.819 ± 0.319	7.363 ± 0.935	7.134 ± 0.855	7.777 ± 0.723	6.310 ± 0.704
Graph GA [†] [30]	10.249 ± 1.002	8.793 ± 0.497	9.211 ± 0.343	8.769 ± 0.432	8.652 ± 0.449	8.900 ± 0.817
SMILES GA [7]	9.334 ± 0.237	8.335 ± 0.276	9.052 ± 0.484	8.560 ± 0.346	8.268 ± 0.170	7.984 ± 0.554
REINVENT [51]	9.867 ± 0.522	8.604 ± 0.483	8.735 ± 0.120	9.054 ± 0.153	8.695 ± 0.370	8.441 ± 0.535
No Feedback (Best-of-N)	6.190 ± 0.821	8.619 ± 0.562	8.230 ± 0.628	8.633 ± 0.549	8.300 ± 0.620	8.793 ± 0.921
Random Feedback	6.604 ± 0.577	8.385 ± 0.258	8.276 ± 0.628	6.780 ± 0.523	8.793 ± 0.921	7.993 ± 0.663
Minimal Feedback	5.863 ± 0.428	8.779 ± 0.633	8.507 ± 0.428	7.998 ± 0.571	9.439 ± 0.922	8.420 ± 0.315
TextGrad [89]	8.531 ± 0.278	8.057 ± 0.383	7.953 ± 0.160	7.256 ± 0.886	8.174 ± 0.395	7.357 ± 0.821
Feedback Descent	10.623 ± 0.112	9.615 ± 0.158	9.919 ± 0.305	10.187 ± 0.253	9.803 ± 0.267	9.300 ± 0.062

Table 6: Full results for molecule optimization on six protein targets with standard deviations. Fragment-based algorithms (denoted by \dagger) operate directly on molecular graphs, giving them structural priors unavailable to purely text-based methods. For each target, the top generative result is in **bold**, and any population in the DOCKSTRING database that exceeds the best generative result is underlined.

- Ground contact or cast shadow for grounding.
- Visible muscle definition suggesting tension/relaxation appropriate to pose.
- Differentiated hair textures: short coat vs coarse mane/tail strands.
- Anatomical landmarks: withers prominence, gaskin curve.

WHAT TO PENALIZE:

- Missing or fused legs; impossible joints; balloon torsos.
- Flat cardboard profiles with no sense of volume.
- Decorative effects that obscure structure.
- Disney-fied proportions (oversized eyes, baby-like features).
- Horn placement anywhere except frontal bone center (2-3" above eye line).

TIEBREAKERS:

- Prefer the image with more accurate limb/neck/head proportions.
- If both are plausible, choose the one with better weight and grounding.

We use the following prompt templates for candidate generation and rationale generation for prompt optimization.

System Prompt Template for Prompt Optimization

Improve the assistant's prompt by extracting actionable insights from the data.

Goal

Create prompts that generalize well beyond the training examples you see here. The patterns below come from a small sample; your output must work on thousands of unseen cases.

Current Prompts

Approach A (Baseline):
'''python

```

{prompt_a_dict}
```
Approach B (Challenger):
```python
{prompt_b_dict}
```
Training Signals
{comparison}

Prompt Improvement Strategy

1. Extract Core Insights
Identify patterns with strong evidence (low p-value, high lift, good support):
- What fundamental strategies distinguish success from failure?
- What misunderstandings or errors repeatedly occur?
- Are there essential facts or constraints the model needs to know?

2. Avoid Common Pitfalls
- Redundancy: Don't say the same thing multiple ways
- Over-specification: Don't list every possible format, constraint, or edge case
- Defensive bloat: Don't add uncertainty handling or safety warnings unless critical
- Surface patterns: Look for deep semantic strategies, not superficial formatting rules
- Enumerationitis: Avoid long numbered checklists; prefer flowing prose

3. Craft Effective Instructions
- State principles clearly and concisely
- Use specific language when precision matters ("identify the missing fact" vs "analyze the information")
- Keep instructions proportional to task complexity
- Test in your mind: would this help on examples you haven't seen?

4. Preserve What Works
- If baseline is effective and simple, make minimal changes
- Don't fix what isn't broken
- Complexity should buy you something measurable

The prompt must be a Python dictionary with the following keys:
{module_keys_description}

Output EXACTLY in this format:

```python
{prompt_template}
```

```

### System Prompt Template for Molecule Optimization

You are a helpful assistant that proposes a single SMILES string corresponding to a small molecule, based on the task explanation and information about previous molecules that have been proposed. Your proposed molecule should score highly on the {benchmark\_name} benchmark.

Task explanation: Maximize  $-\{\text{benchmark\_name}\} - 10 * (1 - \text{QED})$ : larger values mean stronger  $\{\text{benchmark\_name}\}$  binding and high drug-likeness.  
 $\{\text{protein\_info\_xml}\}$

Your output format should be EXACTLY as follows:

```
<reasoning>[Chemical hypothesis linking structural changes to expected binding/QED
improvements]</reasoning>
<smiles>[Single SMILES string]</smiles>
```

Generate a small molecule based on these previous examples (sorted in descending order of score):

$\{\text{examples\_text}\}$

### Example of Protein Metadata (ADRB1)

```
{
 'target': 'ADRB1', 'accession': 'P08588', 'regions': { 'transmembrane': [[56, 84], [94, 120], [133, 154], [173, 196], [223, 248], [320, 349], [355, 377]], 'extracellular': [[1, 55], [121, 132], [197, 222], [350, 354]], 'cytoplasmic': [[85, 93], [155, 172], [249, 319], [378, 477]], 'disordered': [[269, 307], [403, 477]]}, 'critical_residues': {'mutagenesis': {'position': [474, 474], 'description': 'Loss of interaction with GOPC.'}, {'position': [474, 474], 'description': 'Loss of interaction with GOPC; when associated with A-477.'}, {'position': [475, 475], 'description': 'Loss of interaction with GOPC. Loss of interaction with RAPGEF2. Abolishes agonist-induced Ras activation.'}, {'position': [475, 475], 'description': 'Loss of interaction with RAPGEF2.'}, {'position': [475, 475], 'description': 'Partial loss of interaction with GOPC.'}, {'position': [476, 476], 'description': 'Partial loss of interaction with GOPC.'}, {'position': [477, 477], 'description': 'Loss of interaction with GOPC.'}, {'position': [477, 477], 'description': 'Loss of interaction with RAPGEF2. Abolishes agonist-induced Ras activation.'}], 'natural_variants': {'position': [26, 26], 'description': 'in dbSNP:rs34844626'}, {'position': [29, 29], 'description': 'in dbSNP:rs35720093'}, {'position': [31, 31], 'description': 'in dbSNP:rs35230616'}, {'position': [49, 49], 'description': 'correlated with low mean resting heart rate and decreased mortality risk in patients with congestive heart failure; dbSNP:rs1801252'}, {'position': [187, 187], 'description': 'found in individuals with short sleep; results in decreased adenylyl cyclase-activating adrenergic receptor signaling; decreased protein stability; dbSNP:rs776439595.'}, {'position': [389, 389], 'description': 'increased beta1-adrenergic receptor activity; increased basal activity and increased coupling to heterotrimeric G protein Gs that stimulates the adenylyl cyclase; dbSNP:rs1801253.'}, {'position': [399, 399], 'description': 'in dbSNP:rs36052953.'}, {'position': [405, 405], 'description': 'in dbSNP:rs35705839'}]}}}
```

### Example of Molecule Metadata (CCCCC)

```
valid: 'True'
score: '-1.9121449019886678'
metadata:
 CanonicalSMILES: CCCCC
 InChIKey: OFBQJSOFQDEBGM-UHFFFAOYSA-N
```

```
MolecularFormula: C5H12
ExactMass: '72.093900384'
FormalCharge: '0'
AtomCount: '5'
HeavyAtomCount: '5'
HeteroAtomCount: '0'
BondCount: '4'
Sp3CarbonFraction: '1.0'
RingCount: '0'
AromaticRingCount: '0'
AliphaticRingCount: '0'
RotatableBondCount: '2'
StereoCenterCount: '0'
MurckoScaffold: ''
LogP: '2.1965000000000003'
TopologicalPolarSurfaceArea: '0.0'
MolarRefractivity: '25.19899999999999'
HBondDonorCount: '0'
HBondAcceptorCount: '0'
BertzComplexityIndex: '7.5097750043269365'
BalabanJIndex: 2.19060968716425
HallKierAlpha: '0.0'
Kappa1: '5.0'
ChiOv: '4.121320343559642'
TotalESTate: 8.5
MinESTate: 1.34375
MaxESTate: 2.2118055555555554
PEOE_VSA6: '33.10993926815928'
SlogP_VSA5: '33.10993926815928'
BCUTp_1h: '13.744962415414642'
AccessibleSurfaceArea: '34.19901948541599'
FunctionalGroups: []
StructuralAlerts: []
QuantitativeDrugLikeness: '0.4687855098011332'
SyntheticAccessibility: '1.699621281696647'
NaturalProductLikeness: '0.09749981667944'
```